Molecular motions of α-L-rhamnopyranose and methyl α-L-rhamnopyranoside in the glassy and crystalline states: A proton NMR study

ARTICLE *in* PHYSICAL CHEMISTRY CHEMICAL PHYSICS · JULY 2004

Impact Factor: 4.49 · DOI: 10.1039/b402812k

3 AUTHORS:

Huiru Tang
Fudan University
165 PUBLICATIONS **4,933** CITATIONS
SEE PROFILE

Yulan Wang
Chinese Academy of Sciences
132 PUBLICATIONS **4,784** CITATIONS
SEE PROFILE

Peter Belton
University of East Anglia
174 PUBLICATIONS **5,468** CITATIONS
SEE PROFILE

RESEARCH PAPER

PCCP
www.rsc.org/pccp

Molecular motions of α-L-rhamnopyranose and methyl α-L-rhamnopyranoside in the glassy and crystalline states: A proton NMR study

H. R. Tang,†[ac] Y. L. Wang†[a] and P. S. Belton*[b]

[a] *Institute of Food Research, Norwich Research Park, Norwich, UK NR4 7UA*
[b] *School of Chemical Sciences and Pharmacy, University of East Anglia, Norwich, UK NR4 7TJ. E-mail: p.belton@uea.ac.uk; Fax: +44 1603 592003; Tel: +44 1603 593984*
[c] *School of Chemical Sciences, Shaanxi University of Science and Technology, Shaanxi University of Science and Technology, Xianyang, Shaanxi, Peoples Republic of China*

Received 24th February 2004, Accepted 30th March 2004
First published as an Advance Article on the web 4th May 2004

Molecular motions of two saccharides, α-L-rhamnopyranose monohydrate (Rha) and methyl α-L-rhamnopyranoside (Me–Rha) in the crystalline and glassy states have been investigated using proton spin lattice relaxation times, T_1 and $T_{1\rho}$, and transverse relaxation measurements over the temperature range 110–360 K. The results showed that, in all cases, threefold rotational motion of the methoxyl and methyl groups dominate their proton spin–lattice (T_1 and $T_{1\rho}$) relaxation processes at low temperatures. In the crystalline solids the only other process observed to affect $T_{1\rho}$ was water rotation. In the glasses both water rotation and anisotropic rotation of whole sugar molecules was observed. The anisotropic rotation, which was responsible for $T_{1\rho}$ relaxation, gave way to a more isotropic rotation at about 50 K above T_g that was responsible for T_1 relaxation. In general the dynamics of the systems could be described by a model which used discrete correlation times and an Arrhenius temperature dependence for motion. There was no need for recourse to a distribution of correlation times model. The results obtained suggest that both the motion of methyl groups and water are not coupled to the motion of the whole sugar molecules and that a correlation time diagram for the motions of whole molecules above T_g and for water and methyl groups below T_g can be prepared.

Introduction

Saccharides are widespread in almost all animals, plants and microorganisms. They are present in various forms, such as glycoproteins and glycolipids. They account for up to 30% of the dry weight in microorganisms and 80% of that in plants.[1] Plant polysaccharides, including those in starch and plant cell walls, are important in human nutrition, providing humans with a renewable source of energy and fibres. Whilst the polysaccharides in starch can be considered as homopolymers of glucose, in the plant cell walls, the situation is much more complex; homo-polysaccharides and hetero-polysaccharides are entangled together to act as a single unit.[2] Crystalline cellulose fibrils provide a framework and hemicelluloses and pectins, interacting with the fibrils, form a non-crystalline matrix.[2] In addition to polymeric systems, considerable amounts of small saccharides are present and functioning in a non-crystalline state. Carbohydrate glasses have been found in plant seeds, pollen and in the dormant states of desiccation-resistant organisms, where they probably play a protective role.[3] Glassy carbohydrates have also recently found applications in encapsulation and stabilisation of labile therapeutic proteins[4] and pharmaceuticals.[5] α-L-rhamnopyranose (Rha) also known as 6-deoxy-α-L-mannopyranoside, is one of the most important pectic sugars found in the middle lamella and primary cell wall of dicotyledonous plants,[2] where it is often present in the forms of rhamnogalacturonan I and II. Rha plays important roles in both their backbones and side chains.[2] In the backbones, Rha is often in the form of α1,2-linked whereas some side chains are attached to its C4 position.[2] Methyl α-L-rhamnopyranoside is an important synthetic intermediate and a partial structure of a growing family of pyranonaphthoquinone antibiotics,[6–8] which have shown significant antimicrobial and potential antitumor activities.[6,7]

The static structures of these sugars (Fig. 1) have been determined in the forms of α-L-rhamnopyranose monohydrate[9] and methyl α-L-rhamnopyranoside.[10] As a part of our systematic investigation of molecular structure and dynamics in plant polysaccharides and model systems (see for example refs. 11–17), We have studied a number of model sugars related to the components of the plant polysaccharides in the crystalline state. In this paper we report on the comparative behaviour of the dynamics of polycrystalline α-L-rhamnopyranose monohydrate and methyl α-L-rhamnopyranoside, and the same materials in the glassy state.

It has been found that, in polycrystalline carbohydrates, the threefold rotation of methyl groups, re-orientation of water of crystallisation, hydroxyl groups and the *trans-gauche* conformational motions of CH_2O groups[17–21] were the major

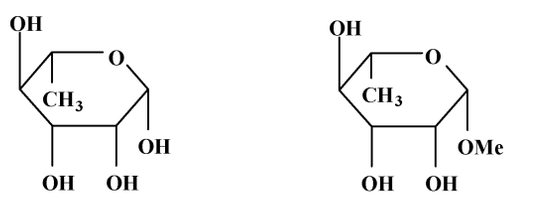

Fig. 1 The structures of rhamnose and methyl rhamnose.

† Present address: Biological Chemistry and Molecular Toxicology Section, Biomedical Sciences Division, Imperial College of Science, Technology and Medicine, Exhibition Road, South Kensington, London, UK SW7 2AZ.

DOI: 10.1039/b402812k

relaxation pathways. No pyran ring puckering or molecular tumbling was detectable in these crystals. Some solid state NMR studies have been reported recently on the maltose–water[22,23] and glucose–water glasses.[24] It has been observed that, below T_g, the restricted motions of CH_2O groups,[23] water and hydroxyl groups[22–24] dominated the NMR relaxation processes whereas, above T_g, the tumbling motions of whole sugar molecules had important contributions as well.[22–24] However the investigations were limited in the range of NMR parameters explored. In this paper we report on the measurement of spin lattice relaxation in the laboratory and rotating frames and second moment across a range of temperatures.

Experimental

Materials

α-L-rhamnopyranose monohydrate (Rha) and methyl α-L-rhamnopyranoside (Me–Rha) were purchased from Sigma and used as the starting materials without further purification. The authenticity of these samples was ascertained by ^{13}C CPMAS spectra. For the D_2O exchanged samples, Rha and Me–Rha were respectively dissolved in sufficient quantity of D_2O (99.9% D) and lyophilised. This process was repeated three times. This process results in the almost complete deuteration of the exchangeable protons (hydroxyl groups and H_2O) of the samples. The samples were then crystallised from fresh D_2O in a sealed desiccator. The crystals so prepared were dried over P_2O_5 for at least 24 h *in vacuo*. This procedure removed excess D_2O from the samples but maintained the α-L-rhamnopyranose as a monohydrate. The samples were all sealed into 5 mm NMR tubes respectively for proton relaxation time measurements.

Preparation of saccharide glasses

Crystalline rhamnose and methyl rhamnoside samples, in both protonated and deuterated forms, were sealed in glass tubes and proton NMR measurements as described below were carried out. The samples were heated to melting point and cooled in an oil bath, this was followed by cooling at room temperature. This process was repeated three times before the next set of proton relaxation time measurements were made. The resultant sugar glasses were transparent and colourless.

Glass transition measurements of the glasses

The thermal transitions of the glasses were recorded using a Perkin–Elmer DSC2 with a heating rate of 10 K min^{-1}. The onset temperature, T_i, was defined as the temperature where the thermogram begins to depart from the baseline. The recovery temperature, T_R, is the temperature at which the thermogram returns to either the initial or a different baseline. The glass transition temperature, T_g, is taken to be the midpoint between the T_i and T_R. The extrapolated onset temperature, T_E, is defined as the temperature at the intersection of the baseline and the tangent to the curve at the point which differs from the baseline, by a value of 1 mW. The peak temperature is the temperature of reversal of the curve.

^1H NMR measurements

Proton spin–lattice relaxation in the laboratory frame, T_1, in the rotating frame, $T_{1\rho}$, and second moment, M_{2r} were measured on a Bruker MSL-100 NMR spectrometer equipped with a proton dedicated probe-head. The sample temperature was controlled with a Bruker variable-temperature unit VT-3000. The experiments were always started from the lowest temperature with 10 K increments; 15 min waiting time after each temperature change was allowed to assure temperature stabilisation and equilibration.

M_{2r} was measured using the solid echo pulse sequence[25] [$90°_x$–τ_1–$90°_y$–τ–AQ] to obtain the complete Bloch decay signal.[26] The 90° pulse length was 1–1.5 μs, τ_1 was 12 μs and τ was chosen to be 4 μs, just slightly longer than the dead time (about 3.5 μs), to ensure observation of an echo. Dwell time was 0.5 μs and recycle delay was $5T_1$. The decay part of the solid echo was fitted to the sum of an exponential and a modified Gaussian function[22,27] to obtain the values of M_{2r}.

T_1 was measured using an inversion–recovery pulse sequence [180°–τ–90°–AQ] with a 90° pulse length of 1–1.5 μs. In order to ensure that the spread of relaxation delays was sufficient to detect multi-exponential relaxation, τ values were chosen by use of the equation $\tau = A \times 10^{(m-1)/12}$, where A is a constant of 1–4 ms depending on the estimated length of T_1, and m is the number of data points. The recycle delay was at least 5 times the proton T_1. Forty-eight data points were measured using a single-point sampling method on the top of the FID 5 μs after the read pulse. The data were fitted to an exponential decay function to obtain the T_1 values.

$T_{1\rho}$ was measured using a standard spin-locking pulse sequence [$90°_x$–τ_{SL}–AQ] where 90° pulse length was 4 μs and spin-locking delay, τ_{SL}, was between 0.4 and 80 ms depending on the length of $T_{1\rho}$. Sixty-four data points were measured using a single-point sampling method on the top of the FID after the spin-lock pulse. The data were then fitted to an exponential decay function to extract $T_{1\rho}$ values.

All relaxation time values were extracted by curve-fitting using a Levenburg–Marquardt non-linear curve-fitting routine installed in TableCurve™ 2D (Jandel Scientific) on a Pentium™ PC.

Results and discussion

Glass transition temperatures

The glass transition processes of the glasses of rhamnopyranose monohydrate and methyl rhamnopyranoside were followed by recording the changes of heat capacity as a function of temperature using DSC. The thermograms in both protonated and deuterated forms are identical. Water content in rhamnopyranose monohydrate is 10.9% (w/w). Its glass transition temperature is about 50 K lower than that of its anhydrous form[28] but only 1 or 2 K lower than that reported[28] for a hydrated sample (10% H_2O). This is consistent with the well-known plasticization effects of water. T_g of Me–Rha is 20 K lower than that of the glasses of the anhydrous rhamnopyranose. This may be due to the fact that it has one hydroxyl group less to participate in hydrogen bonding. Results are given in Table 1.

Proton spin–lattice relaxation in the laboratory frame

Proton spin–lattice relaxation in the laboratory frame of both the crystallised and glassy Rha and Me–Rha in both

Table 1 DSC data for the saccharide glasses

	T_i/K	T_R/K	T_g/K	T_E/K
Rham (H) (monohydrate)	250	270	260	256
Rham(H) anhydrous			310[a]	
Rham(H) (10% water)			262[a]	
Rham (D)	249	272	261	258
Me–Rha (H)	281	298	290	286

[a] Data from ref. 28.

protonated and deuterated forms showed single exponential decay processes over the temperature range studied. The relaxation rates, R_1, of the crystalline materials are plotted *versus* temperature in Fig. 2. For Me–Rha, (Fig. 2b) there is clearly a peak at 180 K and the rise in relaxation rate at lower temperature indicates another maximum at about 110 K, indicating two efficient proton relaxation processes. These correspond to motions of methoxyl and methyl groups. Rha showed one peak at about 180 K, which is due to rotation of the methyl groups. D_2O exchange of both Me–Rha and Rha led to an increase of the relaxation peaks owing to decreased relaxation load after removal of the exchangeable protons in hydroxyl groups and water.

The experimental data were fitted to the well-known Kubo–Tomita expression (eqn. (5)),[13,14,29] assuming exponential correlation functions:

$$R_1 = \frac{1}{T_1} = \sum_{i\geq 1} C_i \left[\frac{\tau_{ci}}{1+\omega_0^2\tau_{ci}^2} + \frac{4\tau_{ci}}{1+4\omega_0^2\tau_{ci}^2} \right] \qquad (1)$$

where ω_0 is the proton Larmor frequency and τ_c the rotational correlation time of the motions responsible for the spin lattice relaxation, which are assumed to follow the Arrhenius activation law

$$\tau_{ci} = \tau_{0i} \exp\left(\frac{E_{ai}}{RT}\right) \qquad (2)$$

where τ_0 is the pre-exponential factor corresponding to the rotational correlation time at infinite temperature, E_a the activation energy and R the gas constant.

C in the eqn. (1) is the relaxation constant. For methyl groups undergoing rapid threefold rotation, C has a relationship with that part of the van Vleck second moment (ΔM_2) modulated by the motions[19,21,30] given in the first part of eqn. (3):

$$C = \frac{2}{3}\Delta M_2 \gamma^2 = \frac{27\gamma^4\hbar^2}{20Nr^6} \qquad (3)$$

C can also be related to, N, the total number of protons relaxed by the methyl group rotation and mean inter-proton distance in the methyl group, r, as given in the second part of eqn. (3). γ is the proton magnetogyric ratio.

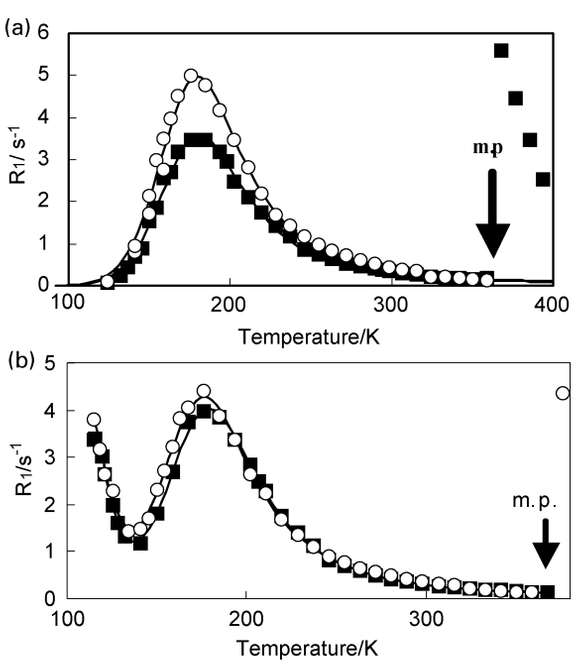

Fig. 2 The spin lattice relaxation rates in the laboratory frame of: (a) rhamnose crystals, (b) methyl rhamnose crystals. Protonated forms: filled squares, deuterated forms open circles. Lines are fits to the data.

For Rha, both the protonated and deuterated samples showed satisfactory agreement between the experimental and fitted data (Fig. 2). The motional parameters obtained from the curve fitting are tabulated in Table 2. Both E_a and τ_0 values are in accord with those for the commonly encountered methyl groups.[16,17,20] Taking the mean r_{H-H} distance[9] in the methyl group of Rha as 1.811 Å, eqn. (3) gives C values as 15.58×10^8 and 27.26×10^8 s^{-2} for protonated and deuterated Rha, respectively. The experimental C value obtained from fitting the data for the protonated Rha (17.56×10^8 s^{-2}) is somewhat larger than the calculated value possibly due to a contribution of dipole–dipole interactions between the methyl and other protons.

For the deuterated Rha, the measured C value (21.95×10^8 s^{-2}) is, however, slightly smaller than the calculated one. This is probably due to incomplete deuteron exchange resulting in a larger value of N than expected.

For Me–Rha data, fitting to a two component form of eqns. (1)–(2) without any constraints showed reasonable agreement between experimental and predicted values (Fig. 2b), relaxation parameters obtained (Table 3) for the high temperature peak (~180 K) showed excellent agreement with those for the methyl groups in a similar environment. However, the low temperature fit due to rotation of the methoxyl group did not yield reliable parameters since the maximum of the relaxation curve was not observed. In order to obtain a fit it was assumed that the C value for the methoxyl group was the same as that for the methyl group. The constrained fitting showed good agreement between the experimental and predicted data. A partially constrained fitting was then carried out in which the value for the methoxy group was fixed and that for the methyl group was allowed to vary. The E_a and τ_0 values so obtained agreed well with those for methoxyl groups in methyl glycosides.[16,20] Comparison of experimental and calculated C values showed the same effects as in the case of Rha.

The motions of the exchangeable protons in hydroxide groups and in water of crystallisation have also been shown[15] to be the proton relaxation pathways. However, in these two sugars, relaxation processes attributable to these were not observed. Hydroxyl groups in the sugars generally provide a weak relaxation mechanism with C values (see refs. 16–18,20 in the order of 1×10^7 s^{-2}. The maximum value of the contribution to the relaxation rate is therefore expected to be about 0.03 s^{-1}. Such a small R_1 peak is expected to be obscured by the dominant contribution to relaxation from the methyl group and thus may not be observed. Reorientation of water molecules may also provide a relaxation mechanism.[20] The calculated C value for the H_2O is about 3.27×10^8 s^{-2}, thus the maximum contribution to relaxation should be slightly greater than 0.9 s^{-1}. This should be observable, provided the activation energy for the motion is not so large as to preclude the rotation rate reaching the required value below the melting point of the crystal. This appears to be the case and this inference is supported by the observation of a high temperature maximum in the $R_{1\rho}$ data (see below). The relaxation rates, R_1, of the glasses are shown in Fig. 3. For rhamnopyranose glass, a relaxation peak is observable at about 185 K (Fig. 3a), attributable to the methyl group. The relaxation of methyl rhamnopyranoside could only be fitted by assuming two peaks at about 120 and 170 K (Fig. 3b), due to rotational motions of CH_3O and CH_3 groups, respectively. However, in both cases, the peaks are much broader than these for the corresponding crystalline sugar.

As in the crystalline sugars D_2O exchange led to an increase in relaxation rates in these peaks (Fig. 3a and b), due to a decreased relaxation load after removal of the exchangeable protons in hydroxyl groups. In contrast to the crystalline

Table 2 Relaxation parameters for α-L-rhamnopyranose crystals from spin–lattice relaxation in the laboratory and rotating frames

	Rha (H)			Rha (D)		
	T_1	$T_{1\rho}$		T_1	$T_{1\rho}$	
Relaxing groups	CH_3–C5	CH_3–C5	H_2O (OHs)	CH_3–C5	CH_3–C5	H_2O(OHs)
Calculated values						
$C_{intra}/10^8$ rad s^{-2}	15.58	15.58	3.27 (0.1[a])	27.26	27.26	—
r_{H-H}/Å[b]	1.811	1.811	1.552	1.811	1.811	—
Experimental values						
E_a/kJ mol^{-1}	12.37 ± 0.21	14.89 ± 0.43[c]	58.3 ± 2.17	12.57 ± 0.18	14.26 ± 0.27[c]	55.83 ± 7.07
$\tau_0/10^{-13}$ s	2.61 ± 0.36	1.38 ± 0.57[c]	$7.14 \pm 5.69(\times 10^{-3})$	2.17 ± 0.26	1.48 ± 0.33[c]	$1.7 \pm 4.3(\times 10^{-2})$
$C/10^8$ rad s^{-2}	15.82 ± 0.22	15.82[c]	4.11 ± 0.11	21.95 ± 0.26	21.95[c]	0.11 ± 0.01
ΔM_2/G^2	3.32 ± 0.05	3.32	0.86 ± 0.02	4.60 ± 0.05	4.60	0.02 ± 0.00
R_{1max}/s^{-1}	3.62	($R_{1\rho max}$) 798[c]	($R_{1\rho max}$) 237	5.04	($R_{1\rho max}$) 1797[c]	($R_{1\rho max}$) 237
Temp. at R_{1max}/K	182	($R_{1\rho max}$) 113[c]	($R_{1\rho max}$) 333[c]	180	($R_{1\rho max}$) 110[c]	($R_{1\rho max}$) 333

[a] Values calculated from data in ref. 9. [b] Average inter-proton distances used in the calculation of C, see text for details. [c] Values predicted from curve-fitting $T_{1\rho}$ data with C constrained to the values obtained from T_1 experiments.

materials, another peak was observed for the glasses at about 70–75 K above their T_g. This peak became smaller upon D_2O exchange (Fig. 3) but did not disappear. Therefore, this peak is provisionally assigned to molecular tumbling motions of the whole molecule with contributions from exchangeable protons and water.

In order to make a direct comparison with the crystalline materials evaluation of the data was initially carried out using the same set of equations and procedures as for the crystalline samples (eqns. (1)–(3)). Despite the assumption of Arrhenius behaviour and a single correlation time, which is generally considered inappropriate for sugar glasses,[24,31] good fits were obtained. For methyl group rotation the E_a and τ_0 values are both within the range of those commonly encountered.[11–17] The least satisfactory fit was obtained with the un-exchanged form of the rhamnose glass. A deviation from the fitted curve can be seen around 280 K. This is probably due to the assumption that motions of water and the whole molecule can be treated as one single process, whereas in fact the motion of the water molecule is slightly separated from the other motions. This idea is supported by the high quality of fit obtained in the anhydrous methyl rhamnose glass and the deuterium exchanged rhamnose glass. The close values of the activation energy and pre-exponential factor for the anhydrous methyl rhamnose and its deuterated form indicate that the hydroxide groups are not moving separately from the whole molecule, in a manner analogous to the methyl groups, but are sharing in the general molecular motion.

An improvement to the fit of the hydrated un-exchanged rhamnose glass data was obtained by using the Cole–Davidson model[32] as expressed in eqn. (4).

$$R_1 = \frac{1}{T_1} = \sum_{i \geq 1} C_i \delta_i \left[\frac{\tau_{ci}}{\sqrt{\left(1+\omega_0^2\tau_{ci}^2\right)^{\delta_i}\left(1+\delta_i^2\omega_0^2\tau_{ci}^2\right)}} + \frac{4\tau_{ci}}{\sqrt{\left(1+4\omega_0^2\tau_{ci}^2\right)^{\delta_i}\left(1+\delta_i^2\omega_0^2\tau_{ci}^2\right)}} \right] \quad (4)$$

In the high temperature data for the rhamnose glass there was significant evidence of a distribution effect. This may be readily explained by the presence of the water motion, which is separate from the overall molecular motion and adds at least one additional correlation time to be accounted for. Although fits were tested in other situations no improvement was observed for any other sample. The general quality of the fits to single correlation time models and the lack of any significant evidence to support distribution of correlation time models indicates that for the motions affecting spin lattice relaxation in the laboratory frame both the assumption of Arrhenius behaviour and single correlation times is appropriate.

Above the melting point of the crystalline species the relaxation rates measured in samples originating from the glassy and crystalline states were identical within experimental error.

Proton spin–lattice relaxation in the rotating frame

Both the crystalline and glassy materials exhibited single exponential decay curves for spin lattice in the rotating frame over

Table 3 Relaxation parameters for methyl α-L-rhamnopyranoside crystals from spin–lattice relaxation in the laboratory and rotating frames

	Me–Rha (H)			Me–Rha (D)		
	T_1	T_1	$T_{1\rho}$	T_1	T_1	$T_{1\rho}$
Relaxing groups	**CH_3**OC^1	**CH_3**–C^{5}H	**CH_3**–C^{5}H	**CH_3**–OC^1	**CH_3**–C^{5}H	**CH_3**–C^{5}H
Calculated values						
$C_{intra}/10^8$ rad s^{-2}	15.58	15.58	15.58	19.83	19.83	19.83
r_{H-H}/Å[a]	1.811	1.811	1.811	1.811	1.811	1.811
Experimental values						
E_a/kJ mol^{-1}	11.8 ± 0.5[b]	12.8 ± 0.2[b]	15.3 ± 0.4[b]	12.7 ± 0.7[b]	12.3 ± 0.2[b]	14.3 ± 0.6[b]
$\tau_0/10^{-13}$ s	$2.4 \pm 1.3(\times 10^{-2})$[b]	1.8 ± 0.2[b]	0.7 ± 0.2[b]	9 ± 7 ($\times 10^{-3}$)[b]	2.2 ± 0.3[b]	1.6 ± 0.9[b]
$C/10^8$ rad s^{-2}	17.73[b]	17.5 ± 0.2[b]	17.56[b]	18.72[b]	18.7 ± 0.2[b]	18.66[b]
ΔM_2/G^2	3.72	3.68 ± 0.04	3.68	3.92	3.91 ± 0.05	3.91

[a] Average proton-carbon distances in the relaxation groups taken from the data for α-L-rhamnopyranose monohydrate. [b] Values predicted with C values constrained as described in the text.

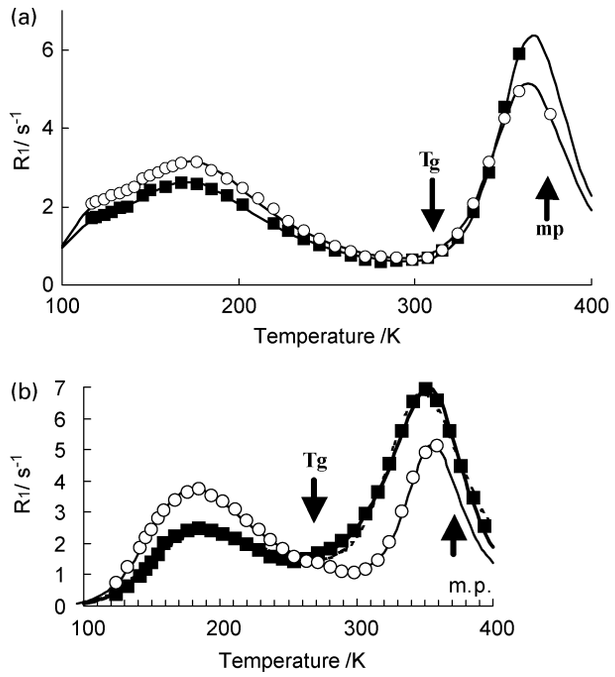

Fig. 3 The spin lattice relaxation rates in the laboratory frame of (a) rhamnose glass, (b) methyl rhamnose glass. Protonated forms: filled squares, deuterated forms open circles. Lines are fits to the data.

the whole temperature range. The relaxation rate $R_{1\rho}$ for the crystalline materials plotted against temperature is shown in Fig. 4. Rha showed two relaxation processes (Fig. 4a) at about 110 and 330 K respectively. D_2O exchange greatly reduced the intensity of the peak at 330 K. This peak must therefore be due to motions of exchangeable protons such as those in the hydroxyl groups and water of crystallisation. For Me–Rha (Fig. 4b), only one relaxation process at low temperature was observed. There was no corresponding high temperature process. Since the Me–Rha is anhydrous but does contain hydroxyl groups it must be concluded that the high temperature peak in Rha arises from water.

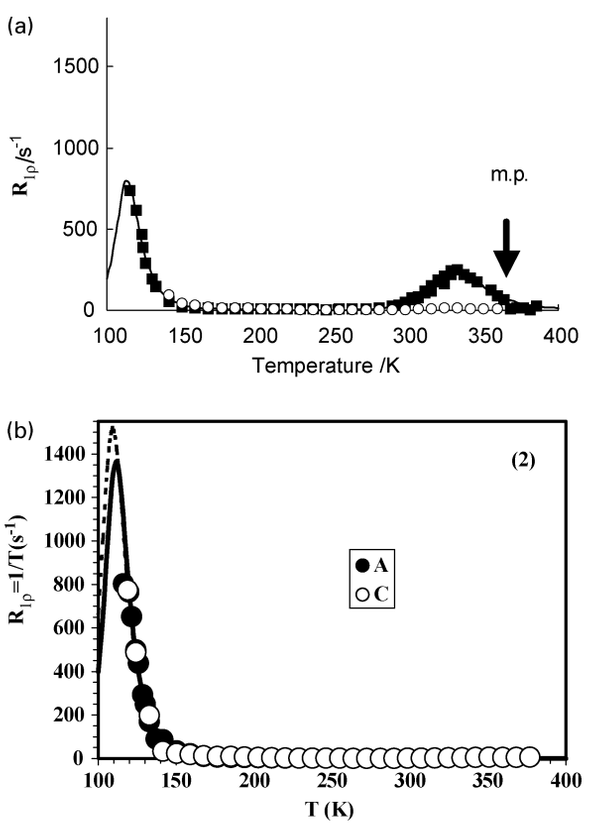

Fig. 4 The spin lattice relaxation rates in the rotating frame of (a) rhamnose crystals (b) methyl rhamnose crystals. Protonated forms: filled squares, deuterated forms open circles. Lines are fits to the data.

The $R_{1\rho}$ data were fitted to an expression similar to that used in R_1 analysis:[16,17]

$$R_{1\rho} = \frac{1}{T_{1\rho}} = \frac{3}{2}\sum_{i\geq 1} C_i\left[\frac{\tau_{ci}}{1+4\omega_{ei}^2\tau_{ci}^2} + \frac{5}{3}\times\frac{\tau_{ci}}{1+\omega_0^2\tau_{ci}^2} + \frac{2}{3}\times\frac{\tau_{ci}}{1+4\omega_0^2\tau_{ci}^2}\right] \quad (5)$$

where ω_0, τ_c and C have the same meaning as in eqn. (1). ω_e is the effective field for relaxation in frequency units, which is generally dependent on both the spin-locking frequency, ω_{SP}, and the local dipolar field (in frequency units), ω_L.

When $\tau_c < T_2$ and $B_{SP} \gg B_L$, where B_L is the local dipolar field and B_{SP} the spin-locking field, $T_{1\rho}$ can be interpreted through the theory of Bloembergen *et al.*[33] therefore, ω_e can be replaced by ω_{SP}. In the current situation, B_{SP} and B_L are of the same order of magnitude (about 67 and 40 kHz respectively) and around the relaxation maximum, $\omega_e\tau_c = 0.55$, hence $\tau_c \leq T_2$. Thus the conditions for the application of BPP theory apply but the effects of the local dipolar field have to be taken into consideration by the McCall–Douglass equation[34]

$$\omega_e = \sqrt{\omega_{SP}^2 + \omega_L^2} \quad (6)$$

In practice, ω_L is temperature dependent. This can be modeled satisfactorily by fitting the second moment data (see below) to a sigmoid function over the temperature range of interest.

$R_{1\rho}$ data for the protonated and deuterated crystalline Me–Rha were fitted to eqns. (5) and (6) (assuming the Arrhenius relationship) as a single process whereas the data for the protonated and deuterated Rha were fitted to a two-process expression. For both sugars, the C value for the low temperature process (90–140 K) was constrained to the values for the methyl group obtained from the T_1 experiments. Under these circumstances maxima are predicted but not observed because of the limits to the temperature range accessible. Parameters obtained are tabulated in Table 4. For both sugars, the E_a values (14–15 kJ mol^{-1}) for the relaxation process at about 110 K confirmed that to be due to the rotation of methyl groups. The C value for the high temperature process (4.11×10^8 s^{-2}) is only slightly greater than that calculated for H_2O (3.7×10^8 s^{-2}) and is thus consistent with the

Table 4 Relaxation parameters for α-L-rhamnopyranose glass from spin–lattice relaxation in the laboratory and rotating frames

	E_a/kJ mol^{-1}	$\tau_0/10^{-12}$ s	$C/10^8$ rad s^{-2}
α-L-Rhamnopyranose glass (H)			
T_1			
CH_3	7.1 ± 0.4	10.8 ± 2.9	10.6 ± 0.4
Mol. and H_2O OHs	42 ± 1.3	4.4 ± 2.0 ($\times10^{-4}$)	27.1 ± 0.5
$T_{1\rho}$			
CH_3	5 ± 1	1800 ± 1900	10.81
H_2O	32 ± 12	0.7 ± 4	2.3 ± 0.5
Mol. and OHs	97 ± 6	1 ± 3 ($\times10^{-11}$)	20.3 ± 0.8
α-L-Rhamnopyranose glass (D)			
T_1			
CH_3	8.0 ± 0.1	4.8 ± 0.3	16.5 ± 0.2
Mol. and H_2O OHs	63 ± 2	5 ± 4 ($\times10^{-7}$)	20.2 ± 0.2
$T_{1\rho}$			
CH_3	7.6 ± 0.8	1.1 ± 0.8	16.50
Mol.	90 ± 2	3 ± 2 ($\times10^{-10}$)	15.1 ± 0.2

deduction that this relaxation process arises because of motion of the water molecules. The relatively large activation energy E_a (55–58 kJ mol^{-1}) for this process may be because all three atoms of the water are involved in a strong hydrogen-bonding network. This high energy also accounts for the failure to observe any corresponding effect in the T_1 data since the required correlation times for effective relaxation would not be reached until above the melting point of the crystal. A scale expansion of the high temperature region showed that a weak peak is present for the D_2O exchanged Rha, confirming an incomplete D_2O exchange discussed in respect of the T_1 experiments.

The relaxation rates, $R_{1\rho}$, for the glasses are shown in Fig. 5. Comparison of the deuterated and protonated rhamnose glasses shows that both exhibit two distinguishable processes at the low and high temperature ends of the experimental range. The low temperature processes may be assigned to methyl group rotation and the high temperature process involves exchangeable protons since the intensity of the maximum is reduced on deuterium exchange. Relaxation cannot be solely due to exchangeable protons however since the change in peak heights is relatively small. It must be concluded therefore that non-exchangeable protons are involved. This in turn implies that motion of the whole molecule must be taking place.

Similar observations were made for the Me–Rha samples and similar conclusions can be drawn. In the case of the protonated Rha another process is observable which contributes to relaxation before the high temperature maximum is reached.

Comparison with the Me–Rha data shows that between about 150 K and 270 K the data for the deuterated and protonated samples do not differ significantly, however for the Rha samples the data for the protonated material begins to deviate at about 150 K and continues to do so. The absence of this effect in the dehydrated sugar suggests that it is due to the motion of water.

As with the R_1 data, the $R_{1\rho}$ data for the glasses were fitted to the BPP model discussed above. During the curve fitting for both the protonated and deuterated methyl rhamnoside glasses, the C values for the low temperature process ($T < 150$ K) were constrained to the values for the methyl group (CH_3) obtained from the T_1 experiments. Parameters obtained are tabulated in Table 5. The E_a values (14–15 kJ mol^{-1}) for the relaxation processes confirmed that to be the rotation of methyl groups.

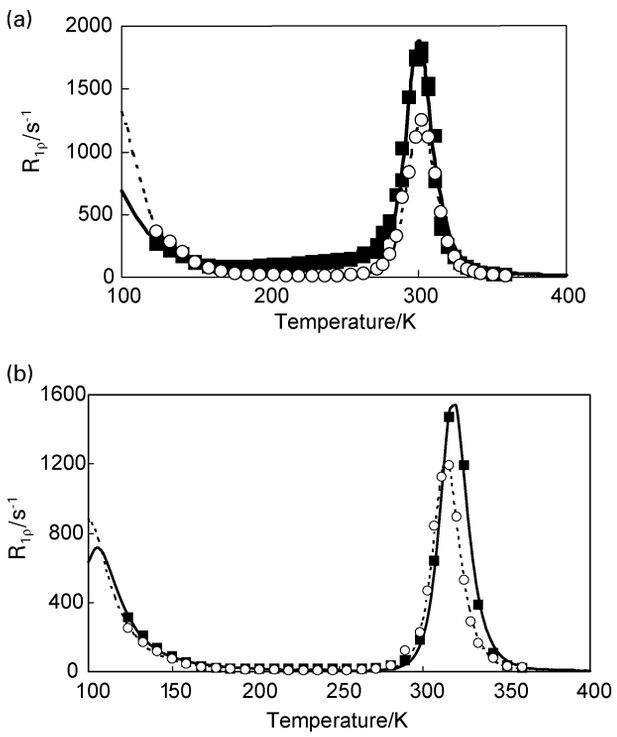

Fig. 5 The spin lattice relaxation rates in the rotating frame of (a) rhamnose glass (b) methyl rhamnose glass. Protonated forms: filled squares, deuterated forms, open circles. Lines are fits to the data.

We note that with one readily explicable exception a simple model involving the Arrhenius law and discrete correlation times is adequate to explain the data. No distribution model is required. There is however a problem with the values of the parameters that describe T_1 and $T_{1\rho}$ for the glasses. The C values for the high temperature rotating frame process is significantly lower than that for the laboratory frame process in all cases, the values of E_a are consistently larger and the values of τ_0 are consistently smaller. This indicates that different motions are involved in both processes. The possibility that it is an artefact of fitting may be discounted by the fact that the effects occur in 4 different independently fitted samples.

If the parameters determined from the R_1 fits are used to predict the $R_{1\rho}$ data a larger maximum at a lower temperature is predicted. Fig. 6a shows an example calculated for methyl rhamnose glass ignoring the effects of methyl and methoxy groups. If it is assumed that both the motions causing laboratory and rotating frame relaxation coexist then a double maximum is predicted (Fig. 6a). On the other hand using rotating frame data to predict the laboratory frame relaxation results in a smaller maximum than observed at higher temperatures. Combining the motion gives rise to a larger maximum. Clearly the motion giving rise to $R_{1\rho}$ maximum cannot persist into the higher temperature region where the R_1 maximum occurs and the motion giving rise to the R_1 maximum cannot persist to much lower temperatures. The transition between these two motions probably occurs in the region of 330 to 340 K. In this region the effects of the motion giving rise to $R_{1\rho}$ maximum adds very little to the observed laboratory frame relaxation rate and the motion giving rise to the R_1 maximum adds very little to the rotating frame relaxation rate. If both motions persisted outside of this region then the data would deviate significantly from the observed results. Presumably the motion observed at the lower temperature is an anisotropic rotation of the molecules and when this rate is of the order of 10^8 s^{-1} there is sufficient thermal energy in the system for the motion to become the more isotropic motion that gives rise to the R_1 maximum.

Proton second moments

In order to describe the transverse relaxation behaviour of both crystalline and glassy samples over the whole temperature

Table 5 Relaxation parameters for methyl α-L-rhamnopyranoside glass from spin–lattice relaxation in the laboratory and rotating frames

	E_a/kJ mol^{-1}	$\tau_0/10^{-12}$ s	$C/10^8$ rad s^{-2}
Methyl α-L-rhamnopyranose glass (H)			
T_1			
CH_3O	6 ± 3	4 ± 11	6. ± 1
CH_3	9 ± 1	3 ± 2	9 ± 3
Mol. and OHs	67 ± 2	2 ± 2(×10^{-7})	27 ± 0.9
$T_{1\rho}$			
CH_3	8.3 ± 0.9	79 ± 63	9.31
Mol. and OHs	114 ± 2	1.6 ± 1.5 (×10^{-13})	17.8 ± 0.3
Methyl α-L-rhamnopyranose glass (D)			
T_1			
CH_3O	6 ± 2	2 ± 5	8.2 ± 0.8
CH_3	9 ± 1	2 ± 1	11 ± 2
Mol. and OHs	61 ± 1	1.7 ± 0.8 (×10^{-6})	21.3 ± 0.3
$T_{1\rho}$			
CH_3	8.1 ± 0.8	63 ± 49	20.21
Mol. and OHs	114 ± 2	1.1 ± 0.1(×10^{-13})	13.8 ± 0.2

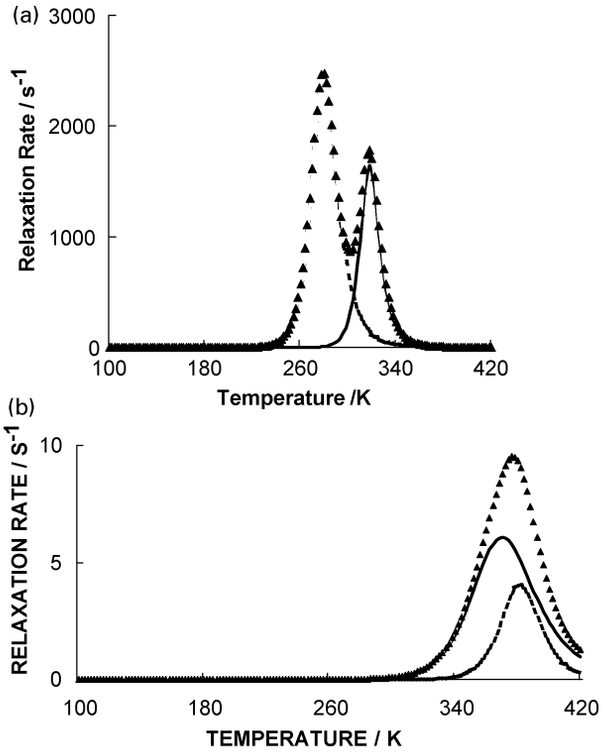

Fig. 6 Predicted and observed values for (a) spin lattice relaxation in the rotating frame for methyl rhamnose: dark line calculated from observed $R_{1\rho}$ data, dotted line calculated from observed R_1 data, light line containing triangles calculated combined rates (b) spin lattice relaxation in the laboratory frame for methyl rhamnose: dark line calculated from observed R_1 data, dotted line calculated from observed $R_{1\rho}$ data, light line containing triangles calculated combined rates. See text for details of the calculation.

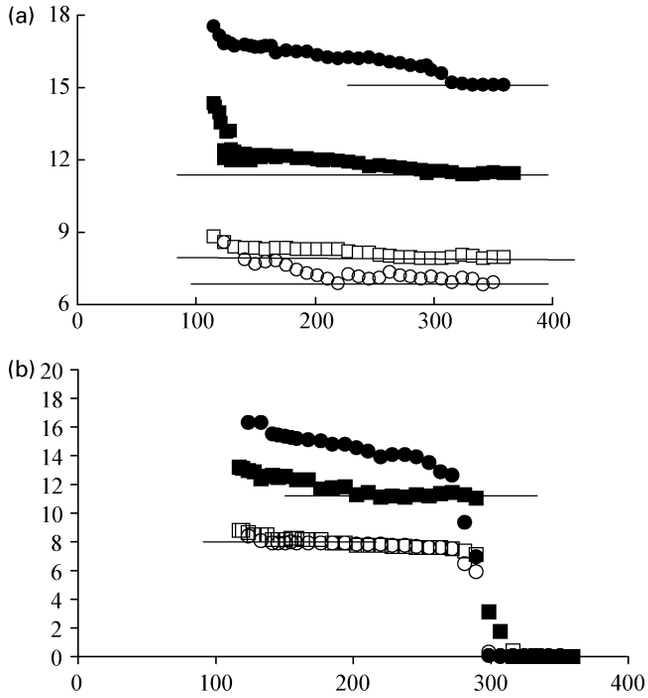

Fig. 7 (a) Variation of rigid lattice second moment with temperature for: rhamnose crystals, protonated form, filled circles, deuterated form, open circles. Methyl rhamnose crystals, protonated form, filled squares, deuterated form, squares. Horizontal lines indicate plateau regions. (b) Variation of rigid lattice second moment with temperature for: rhamnose glass, protonated form, filled circles, deuterated form, open circles; methyl rhamnose glass, protonated form, filled squares, deuterated form, squares. Horizontal lines indicate plateau regions.

range a sum of an exponential and a modified Gaussian function[27] as shown in eqn. (7) was used.

$$I(t) = I_G \exp\left(\frac{-a^2t^2}{2}\right)\frac{\sin bt}{bt} + I_E \exp\left(-\frac{t}{T_{2E}}\right) \quad (7)$$

The residual rigid lattice second moment is defined as $M_{2r} = a^2 + b^2/3$. In general, M_{2r} will decrease in value when the motions of some of the protons contributing to the local field have a correlation time, τ_c, which is comparable to the inverse of line-width,

$$i.e., \qquad \tau_c \leq \left(\gamma\sqrt{M_{2r}}\right)^{-1} \quad (8)$$

The line narrowing transition is expected to be complete when $\left(\gamma\sqrt{M_{2r}}\right)\tau_c \ll 1$. For the glasses, below the T_g, there was no exponential component contribution to relaxation. During the glass transition processes, both components were observed and the relative ratio, I_G/I_E, decreased as temperature increased. At 40–50 K above the T_g, the Gaussian component vanished due to fast molecular motions and only the exponential component was observable. In the case of the crystalline components I_E was zero over the temperature range measured

The temperature dependence of M_{2r} for the protonated and deuterated crystalline Rha and Me–Rha is shown in Fig. 7a. For the protonated Rha, a plateau is around 15.2 G^2 (315–350 K). Below 140 K there is a sharp increase in second moment, above this to 315 K there is a gradual decrease in M_{2r}. At around 140 K the value of M_{2r} is 16.6 G^2. The rigid lattice M_{2rigid} value, calculated from the lattice summation[49], is 19.9 G^2. Using eqn. (8) and the experimental relaxation constant, C, for methyl rotation, the reduction in the total second moment due to methyl group motion is 3.4 G^2. This value is therefore consistent with the value of 16.6 G^2 observed above 140 K. The calculated M_{2r} reduction resulting from motions of water and hydroxyl groups are 0.88 and 0.23 G^2 respectively. Therefore, the overall M_{2r} reduction of 1.4 G^2 between 140 and 350 K is therefore assigned to the combined motional effects of hydroxyl groups and water. This is in agreement with the observation of a maximum in $R_{1\rho}$ at 333 K due to water and suggests that the high temperature plateau arises due to residual static interactions remaining after the motion of water and methyl groups have entered the motional narrowing regime.

For Me–Rha, the total rigid lattice second moment is calculated[30] by summation to be 19.8 G^2. The part of the second moment modulated by the rotation of methoxy and methyl groups together is calculated from the experimental data to be 7.4 G^2 The value of 11.6 G^2 observed above 140 K is thus consistent with the calculated values in the presence of methyl and methoxy group rotation. Thereafter the value of the second moment declines gradually. As in the case of Rha the plateau observed may be attributed to residual static interactions.

The deuterated Rha and Me–Rha have shown much smaller M_{2r} over the whole temperature region compared with their protonated forms. This can be explained by the reduction of (proton) spin density after removal of exchangeable protons. The only relatively sharp M_{2r} reduction for these two samples appeared to be that resulting from the methyl rotation.

The temperature dependence of M_{2r} for the sugar glasses is shown in Fig. 7b. Two sharp M_{2r} reductions may be seen in the protonated Rha at 140 K and 265 K. In Me–Rha a smaller change is seen at about 140 K and a sharp decrease is observed at 295 K (Figs. 4a and c). Similar effects are seen in the deuterated samples. The changes at about 140 K correspond to the

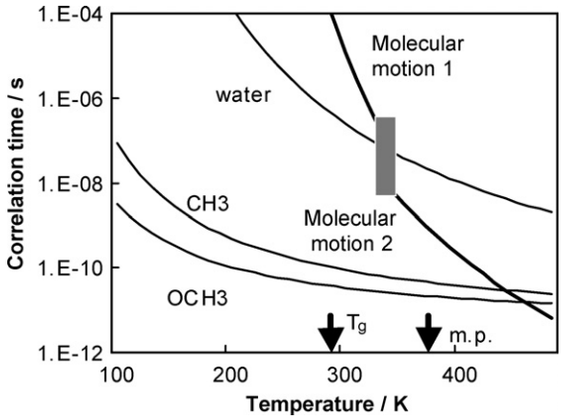

Fig. 8 Calculated correlation times for a hypothetical hydrated methyl rhamnose glass. Molecular motion 1 is the motion giving rise to the observed spin lattice relaxation in the rotating frame; molecular motion 2 is the motion giving rise to spin lattice relaxation in the laboratory frame. The shaded area is where the transition from one motion to another occurs (see Table 1 for DSC data for the saccharide glasses).

threefold motional effects of methyl (and in Me–Rha, methoxy) groups. The high temperature M_{2r} reductions, at 270 K for Rha and 295 K for Me–Rha glasses, coincided with the glass transition temperature and are associated with the effects of molecular tumbling. Using eqn. (8) the motional correlation time at T_g is estimated to be 30–40 μs.

Since the reliable data for the inter-proton distances in the glasses are not available, their rigid lattice M_{2rigid} values cannot be calculated from the lattice summation. However, combining the experimental values of the plateaux at 140–170 K and the relaxation constants from the T_1 and $T_{1\rho}$ data a value of the rigid lattice M_{2r} can be estimated. For Rha this is 19.8 G^2 and for Me–Rha it is 19.8 G^2. These values are very close to those for the crystalline material.

Conclusions

A number of different processes are present in the crystalline materials and glasses. In both cases methyl group rotation appears to be relatively uncoupled to the motions of the rest of the system. In particular no evidence of a distribution of correlation times of the methyl groups was observed in the glasses. Water motions fast enough to give rise to $R_{1\rho}$ maxima in the hydrated crystals and glasses can be observed below the melting point in the case of the crystals and below T_g in the hydrated glass. So again these motions appear to be only weakly coupled to the rest of the system. No whole molecule motion was observed below the melting point for the crystalline materials but it was observed in the glasses. Significant motion occurs above T_g, which is anisotropic and undergoes a transition to more isotropic motion about 50 K above T_g. The analysis of motions allows the construction of a correlation time diagram for the glass. This is shown in Fig. 8.

Acknowledgements

BBSRC is thanked for the part funding of this work under its competitive strategic grant scheme.

References

1 T. Sheng, *Biochemistry*, PKU Press, Beijing, 1994.
2 C. T. Brett and K. W. Waldron, *The Physiology and Biochemistry of Plant Cell Walls*, Unwin Hyman, London, 1990.
3 J. H. Crowe, J. F. Carpenter and L. M. Crowe, *Ann. Rev. Physiol.*, 1998, **60**, 73–103.
4 J. L. Cleland and R. Langer, *Formulation and Delivery of Proteins and Peptides*, ACS, Washington, 1994.
5 S. L. Shamblin, X. L. Tang, L. Q. Chang, B. C. Hancock and M. J. Pikal, *J. Phys. Chem. B*, 1999, **103**, 4113–4121.
6 P. Krishnan and K. F. Bastow, *Cancer Chemother. Pharmacol.*, 2001, **47**, 187–198.
7 M. A. Brimble, L. J. Duncalf and M. R. Nairn, *Nat. Prod. Rep.*, 1999, **16**, 267–281.
8 M. A. Brimble, M. R. Nairn and H. Prabaharan, *Tetrahedron*, 2000, **56**, 1937–1992.
9 S. Takagi and G. A. Jeffrey, *Acta Crystallogr., Sect. B: Struct. Crystallogr. Cryst. Chem.*, 1978, **B34**, 2551–2555.
10 M. A. Shalaby, F. R. Fronczek and E. S. Younathan, *Carbohydr. Res.*, 1994, **258**, 267–274.
11 I. J. Colquhoun, R. Parker, S. G. Ring, L. Sun and H. R. Tang, *Carbohydr. Polym.*, 1995, **27**, 255–259.
12 H. R. Tang, J. Godward and B. Hills, *Carbohydr. Polym.*, 2000, **43**, 375–387.
13 H. R. Tang, Y. L. Wang and P. S. Belton, *Solid State NMR*, 2000, **15**, 239–248.
14 H. R. Tang, P. S. Belton, S. C. Davies and D. L. Hughes, *Carbohydr. Res.*, 2001, **330**, 391–399.
15 B. P. Hills, Y. L. Wang and H. R. Tang, *Mol. Phys.*, 2001, **99**, 1679–1687.
16 Y. L. Wang, H. R. Tang and P. S. Belton, *J. Phys. Chem. B*, 2002, **106**, 12 834–12 840.
17 H. R. Tang and P. S. Belton, *Solid State NMR*, 2002, **21**, 117–133.
18 E. C. Reynhardt and L. Latanowicz, *Chem. Phys. Lett.*, 1996, **251**, 235–241.
19 L. Latanowicz, E. C. Reynhardt, R. Utrecht and W. Medycki, *Ber. Bunsen-Ges. Phys. Chem.*, 1995, **99**, 152–157.
20 H. R. Tang and P. S. Belton, *Solid State NMR*, 1998, **12**, 21–30.
21 L. Latanowicz and E. C. Reynhardt, *Ber. Bunsen-Ges. Phys. Chem.*, 1994, **98**, 818–823.
22 I. J. van den Dries, D. van Dusschoten and M. A. Hemminga, *J. Phys. Chem. B*, 1998, **102**(51), 10 483–10 489.
23 R. H. Tromp, D. van Dusschoten, R. Parker and S. G. Ring, *Phys. Chem. Chem. Phys.*, 1999, **1**, 1927–1931.
24 G. R. Moran and K. R. Jeffrey, *J. Chem. Phys*, 1999, **110**, 3472–3483.
25 J. G. Powles and P. Mansfield, *Phys. Lett.*, 1962, **2**, 58–59.
26 J. G. Powles and J. H. Strange, *Proc. Phys. Soc.*, 1963, **82**, 6–15.
27 A. Abragam, *The Principles of Nuclear Magnetism*, Oxford University Press, 1961.
28 T. R. Noel, R. Parker and S. G. Ring, *Carbohydr. Res.*, 2000, **329**, 839–845.
29 R. Kubo and K. Tomita, *J. Phys. Soc. Jpn.*, 1954, **9**, 888–919.
30 J. H. van Vleck, *Phys. Rev.*, 1948, **74**, 1168–1183.
31 M. D. Ediger, *Annu. Rev. Phys. Chem.*, 2000, **51**, 99–128.
32 E. R. Andrew, R. Gaspar and W. Vennart, *Biopolymers*, 1978, **17**, 1913–1925.
33 N. Bloembergen, E. M. Purcell and R. V. Pound, *Phys. Rev.*, 1948, **73**, 679–712.
34 D. W. McCall and D. C. Douglass, *Appl. Phys. Lett.*, 1965, **7**, 12–14.